The reconstructed Indonesian warm pool sea surface temperatures from tree rings and corals: Linkages to Asian monsoon drought and El Niño–Southern Oscillation

Citation for published version:
D'Arrigo, R, Wilson, R, Palmer, J, Krusic, P, Curtis, A, Sakulich, J, Bijaksana, S, Zulaikah, S, Ngkoimani, LO & Tudhope, A 2006, 'The reconstructed Indonesian warm pool sea surface temperatures from tree rings and corals: Linkages to Asian monsoon drought and El Niño–Southern Oscillation', *Paleoceanography*, vol. 21, no. 3, PA3005, pp. 1-13. https://doi.org/10.1029/2005PA001256

Digital Object Identifier (DOI):
10.1029/2005PA001256

Published In:
Paleoceanography

The reconstructed Indonesian warm pool sea surface temperatures from tree rings and corals: Linkages to Asian monsoon drought and El Niño–Southern Oscillation

Rosanne D'Arrigo,[1] Rob Wilson,[2] Jonathan Palmer,[3] Paul Krusic,[1] Ashley Curtis,[1] John Sakulich,[1] Satria Bijaksana,[4] Siti Zulaikah,[4] La Ode Ngkoimani,[5] and Alexander Tudhope[2]

Received 7 December 2005; revised 29 March 2006; accepted 19 April 2006; published 9 August 2006.

[1] The west Pacific warm pool is the heat engine for the globe's climate system. Its vast moisture and heat exchange profoundly impact conditions in the tropics and higher latitudes. Here, September–November sea surface temperature (SST) variability is reconstructed for the warm pool region (15°S–5°N, 110–160°E) surrounding Indonesia using annually resolved teak ring width and coral $\delta^{18}O$ records. The reconstruction dates from A.D. 1782–1992 and accounts for 52% of the SST variance over the most replicated period. Significant correlations are found with El Niño–Southern Oscillation (ENSO) and monsoon indices at interannual to decadal frequency bands. Negative reconstructed SST anomalies coincide with major volcanic eruptions, while other noteworthy extremes are at times synchronous with Indian and Indonesian monsoon drought, particularly during major warm ENSO episodes. While the reconstruction adds to the sparse network of proxy reconstructions available for the tropical Indo-Pacific, additional proxies are needed to clarify how warm pool dynamics have interacted with global climate in past centuries to millennia.

Citation: D'Arrigo, R., R. Wilson, J. Palmer, P. Krusic, A. Curtis, J. Sakulich, S. Bijaksana, S. Zulaikah, L. O. Ngkoimani, and A. Tudhope (2006), The reconstructed Indonesian warm pool sea surface temperatures from tree rings and corals: Linkages to Asian monsoon drought and El Niño–Southern Oscillation, *Paleoceanography*, *21*, PA3005, doi:10.1029/2005PA001256.

1. Introduction

[2] Ocean-atmosphere variability associated with the equatorial western Pacific warm pool impacts climate worldwide [*Wang and Xie*, 1998; *Barlow et al.*, 2002; *Sun*, 2003]. Tropical warm pool waters surrounding the Indonesian maritime continent feature some of the highest (>28.5°C) sea surface temperatures (SSTs) on Earth. Heat and water vapor are transported from the warm pool to higher latitudes via deep convective clouds and the prevailing atmosphere-ocean circulation. Even small changes in warm pool SST can have substantial consequences for global climate (e.g., for tropical cyclone activity [*Emanuel*, 2005]). Warm pool conditions, modulated by the El Niño–Southern Oscillation (ENSO) system, reverberate around the globe. Recent central and southwest Asian drought, for example, was attributed to an enhanced signal in the warm pool region associated with ENSO [*Barlow et al.*, 2002]. In turn, shifts in warm pool SST can modulate ENSO variability [*Sun*, 2003]. However, these relationships are very complex and a partial decoupling of warm pool conditions from the ENSO system can occur due to a variety of influences [*Schneider*, 1998; *Hoerling et al.*, 2001].

[3] Increasingly, paleoclimatic records are being applied to extend our understanding of tropical climate variability, including ENSO, into the past. For example, reconstructions based primarily on tree rings have been developed for ENSO indices [*Stahle et al.*, 1998; *Mann et al.*, 2000; *D'Arrigo et al.*, 2005a]. However, much of the data on which these reconstructions are based originate from subtropical North America, and therefore rely on teleconnected relationships with ENSO rather than a direct influence from the tropics. Coral-based climate records have been used to reconstruct ENSO-related changes in SST and salinity in the Indo-Pacific [*Charles et al.*, 1997; *Cole et al.*, 2000; *Evans et al.*, 2002; *Cobb et al.*, 2003; *Linsley et al.*, 2004] and for the west Pacific warm pool during glacial and interglacial time periods [*Tudhope et al.*, 2001]. Coral records have also been related to Pacific decadal variability [*Linsley et al.*, 2000; *Cobb et al.*, 2001; *Evans et al.*, 2001; *D'Arrigo et al.*, 2005b], and used to assess dynamics between the Indian and Pacific Oceans [*Cole et al.*, 2000; *Charles et al.*, 2003]. However, large-scale, continuous tropical climate reconstructions are still relatively rare [*Evans et al.*, 2002; *Wilson et al.*, 2006]. Below we describe a reconstruction of Indonesian warm pool SSTs that is derived from tree ring

[1] Tree Ring Laboratory, Lamont-Doherty Earth Observatory, Palisades, New York, USA.
[2] School of Geosciences, University of Edinburgh, Edinburgh, UK.
[3] Department of Archaeology and Palaeoecology, Lincoln University, Canterbury, New Zealand.
[4] Department of Physics, Bandung Technical University, Bandung, Indonesia.
[5] Jurusan Fisika, Universitas Haluoleo, Sulawesi, Indonesia.

0883-8305/06/2005PA001256

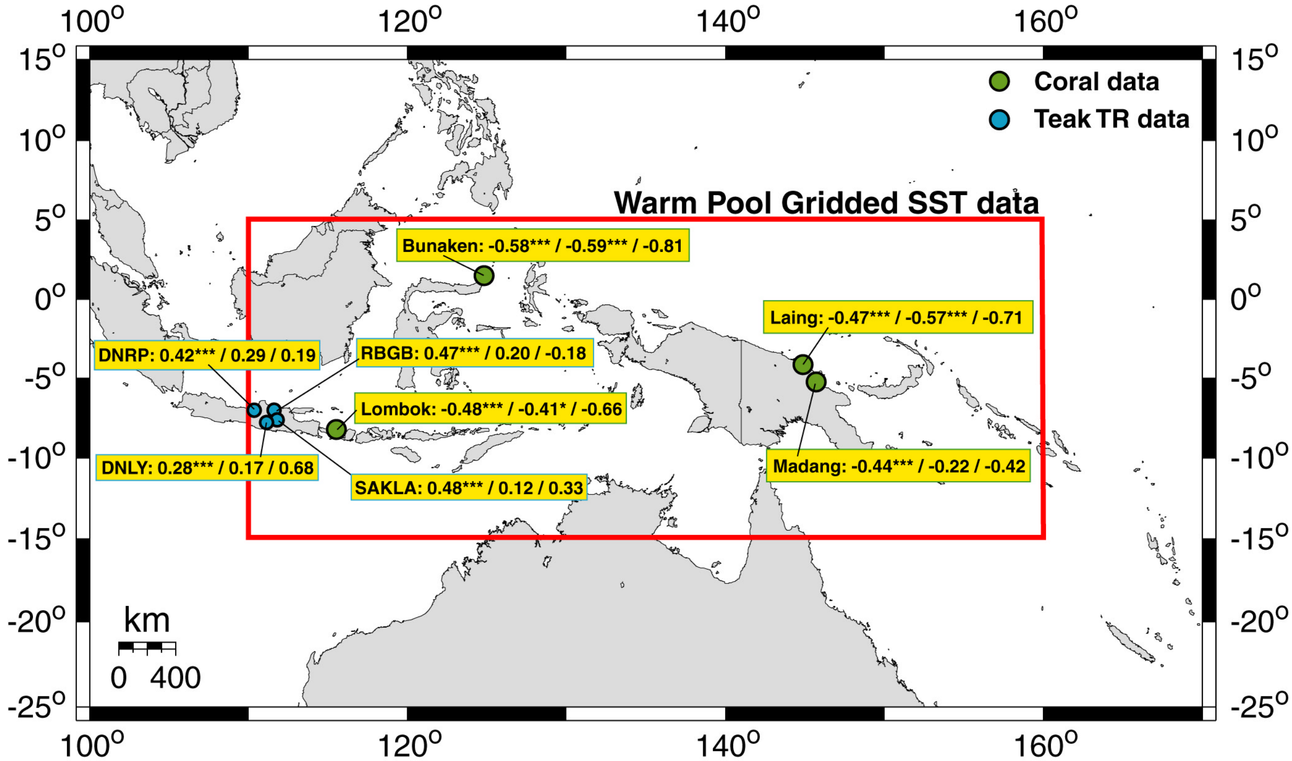

Figure 1. Map of Indonesian warm pool region (15°S–5°N, 110–160°E) showing locations of four tree ring [*D'Arrigo et al.*, 1994] and four coral $\delta^{18}O$ records [*Moore*, 1995; *Charles et al.*, 2003; *Tudhope et al.*, 2001] that were used as candidate predictors for the warm pool reconstruction. These coral records are independent of those used in a recent reconstruction of tropical temperatures (see text; and *Wilson et al.* [2006]). The chronologies of individual corals are based on annual banding in skeletal density and geochemistry. The excellent zero-lag match between the coral $\delta^{18}O$ records and ENSO indices throughout their length suggests that they are precise to within a year, but, conservatively, we could assess the maximum age uncertainty as ±2 years over the length of each record. The values show the correlations, calculated over 1885–1989, between the proxy and the September–November season of the warm pool SSTs for three frequency bands (<10, 10–30, and >30 years). The degrees of freedom have been adjusted to account for the first-order autocorrelation in the time series [*Dawdy and Matalas*, 1964]. The resultant significance of the correlations is denoted by one, two, or three asterisks for the 90%, 95%, or 99% confidence limits, respectively.

and coral proxies, and evaluate its relation to other features of the tropical climate system.

2. Warm Pool SST Reconstruction From Tree Rings and Corals

[4] Monthly gridded SST data were extracted from the *Kaplan et al.* [1998] data set for the warm pool region in the vicinity of Indonesia and averaged over the area bounded by the coordinates 15°S–5°N; 110°–160°E (i.e., an average of 40 grids, Figure 1). This area was selected because it encompasses much of the warm pool region associated with the Indonesian Low (a center of action of the ENSO system), while also optimizing the signal between the SST and proxy data. It should be noted, however, that the spatial extent of the warm pool waxes and wanes for a variety of reasons (http://earthobservatory.nasa.gov/Study/WarmPool/) and that here we reconstruct SSTs for an area within the warm pool region rather than for the warm pool per se.

[5] A data set of 12 teak (*Tectona grandis*) ring width records has been developed for Indonesia over the past two decades (Table 1) [*D'Arrigo et al.*, 1994; *Cook et al.*, 2000]. The teak chronologies were processed by detrending the raw ring width series, after they had been power transformed [*Cook and Peters*, 1997], with negative exponential or linear negative/zero slope functions. Many of these teak records correlate significantly with indices of ENSO, consistent with the tendency for warm ENSO events to be linked with drought and decreased teak growth in Indonesia [*D'Arrigo et al.*, 1994; *Cook et al.*, 2000]. One of the teak records, Saradan, was previously included in a tree ring reconstruction of the Southern Oscillation Index (SOI [*Stahle et al.*, 1998]). Many of the teak ring width series represent new or updated chronologies, and due to low replication at some of the sites (Table 1) and the close proximity of these sites, regional clusters of tree ring data were composited together to develop more robust mean functions. Screening the teak chronologies against the

Table 1. Description of the Teak Ring Width Chronologies and Coral Series[a]

Site Name	Site Code	Latitude, deg	Longitude, deg	Full Period	Number of Series	Mean r	Period > 10 Series
			Individual Chronologies				
Randublatung	RAN	7.06 S	111.22 E	1925–2004	13	0.47	1938–2004
Bekutuk	BEK	7.07 S	111.22 E	1668–2004	20	0.40	1834–2004
Gubug Payung	GUB	7.05 S	111.29 E	1864–2004	18	0.34	1879–2004
Pangaran Natural Forest	PGR	7.29 S	111.48 E	1815–2004	9	0.46	-
Donoloyo Cagar Alam	DNLY	7.52 S	111.12 E	1714–2004	13	0.39	1746–2004
Pagerwunung Darupono	DNRP	7.02 S	110.16 E	1776–2004	19	0.39	1820–2004
Klangon Natural Forest	KLA	7.30 S	111.47 E	1707–2004	15	0.49	1812–2004
Saradan	SAR	7.29 S	111.42 E	1689–2000	30	0.46	1812–2000
Sepanjang	SPJ	7.00 E	115.30 E	1760–2000	35	0.49	1834–2000
Bigin	BIG	7.10 S	111.34 E	1839–1995	20	0.59	1853–1995
Muna	MUN	5.30 S	123.00 E	1564–1995	39	0.42	1673–1994
Cepu	CEP	7.30 S	110.00 E	1870–1991	13	0.45	1896–1991
			Composite Series				
SAKLA	SAKLA	-	-	1689–2004	45	0.46	1759–2004
RBGB	RBGB	-	-	1668–2004	71	0.36	1834–2004
			Coral Series				
Lombok Strait	LOM	8.15 S	115.30 E	1782–1990	-	-	-
Bunaken	BUN	1.30 N	124.50 E	1860–1989	-	-	-
Madang Lagoon	MAD	5.13 S	145.49 E	1881–1992	-	-	-
Laing Island	LNG	4.09 S	144.53 E	1885–1992	-	-	-

[a]Mean r is the mean interseries correlation between the series as derived from program COFECHA [*Holmes*, 1983]. SAKLA is a composite of KLA and SAR; RBGB is a composite of RAN, BEK, GUB, and BIG.

gridded warm pool SST data identified four chronologies (two of which are composites, Figures 1 and 2 and Table 1) that express significant (99% confidence limit (CL)) correlations, at high frequencies, with the instrumental data and were considered for further analysis.

[6] In the vicinity of the western Pacific warm pool (from Indonesia, New Guinea, and the Cape York region of Australia), there exist nine 100-year-long, annually resolved coral records (four skeletal δ^{18}O and five calcification series) measured from massive *Porites* with a maximum age uncertainty of ±2 years in their early portions. Of these, the four δ^{18}O records (annualized but otherwise unprocessed) showed significant high-frequency correlations (99% CL) with warm pool SSTs and were selected for use in this study (Figure 1). As with the teak chronologies, these coral records, from Bunaken (Sulawesi Sea) and Lombok Strait [*Moore*, 1995; *Charles et al.*, 2003]; and Laing Island and Madang Lagoon (New Guinea [*Tudhope et al.*, 2001]), demonstrate significant relationships with ENSO but are also subject to local effects; it is important to note that we are only reconstructing SSTs rather than ENSO or other indices specifically. Reflecting the general spatially heterogeneous signal of SSTs through our defined warm pool grid, the Lombok series is more sensitive to easternmost Indian Ocean conditions, while the Bunaken, Laing, and Madang sites display strong correlations with both warm pool SSTs and Darwin, Australia sea level pressure (SLP), and are sensitive to local as well as regional-scale western Pacific conditions (Figures 1 and 2) [*Moore*, 1995; *Tudhope et al.*, 2001]. We should note, however, that coral isotopic δ^{18}O portrays a mixture of temperature and water composition (salinity) changes, although in the warm pool these variables often correlate positively with each other since most of the rainfall is related to deep atmospheric convection consequent on heating from below [*Charles et al.*, 2003; *Lough*, 2004]. Our own analyses (not shown) indicate that the relationships between the coral δ^{18}O records, SST, and salinity are reasonably consistent at the frequencies defined herein, implying that temperature is the dominating control on δ^{18}O for those records used. To try and identify potential biases in the frequency domain from conflicting influences of SST and salinity, the correlations undertaken to screen the data were calculated for three frequency bands (<10, 10–30 and >30 years, Figure 1). For the coral records, the sign of the correlations is the same at each frequency band, with the strongest correlations generally at lower frequencies. We should note though that when the degrees of freedom are corrected for first-order autocorrelation in the smoothed series [*Dawdy and Matalas*, 1964], correlations at timescales >30 years are not significant even at the 90% CL. However, at the midfrequencies (10–30 years), significant correlations (>90% CL) are noted for Lombok, Bunaken and Laing. The frequency-dependent correlations derived for the tree ring data are more variable, suggesting that more care is needed in using these (land-based) data for a reconstruction of warm pool SSTs. This is addressed in more detail below.

[7] Because of the relatively small number of proxy time series and the relatively low interseries correlations (Table 2), rather than using principal component regression, stepwise multiple regression (F-to-enter is 0.05; F-to-remove is 0.10) was used to develop the reconstruction. This approach allows only those proxy series that most significantly represent the instrumental data to enter the regression

Figure 2. Teak and coral records that correlate significantly with warm pool SSTs (Figure 1). The series were normalized to the common period (note that the sign of the coral series is reversed). The smoothed function is a 15-year spline. (top) Proxy records used and (bottom) not used for the warm pool reconstruction.

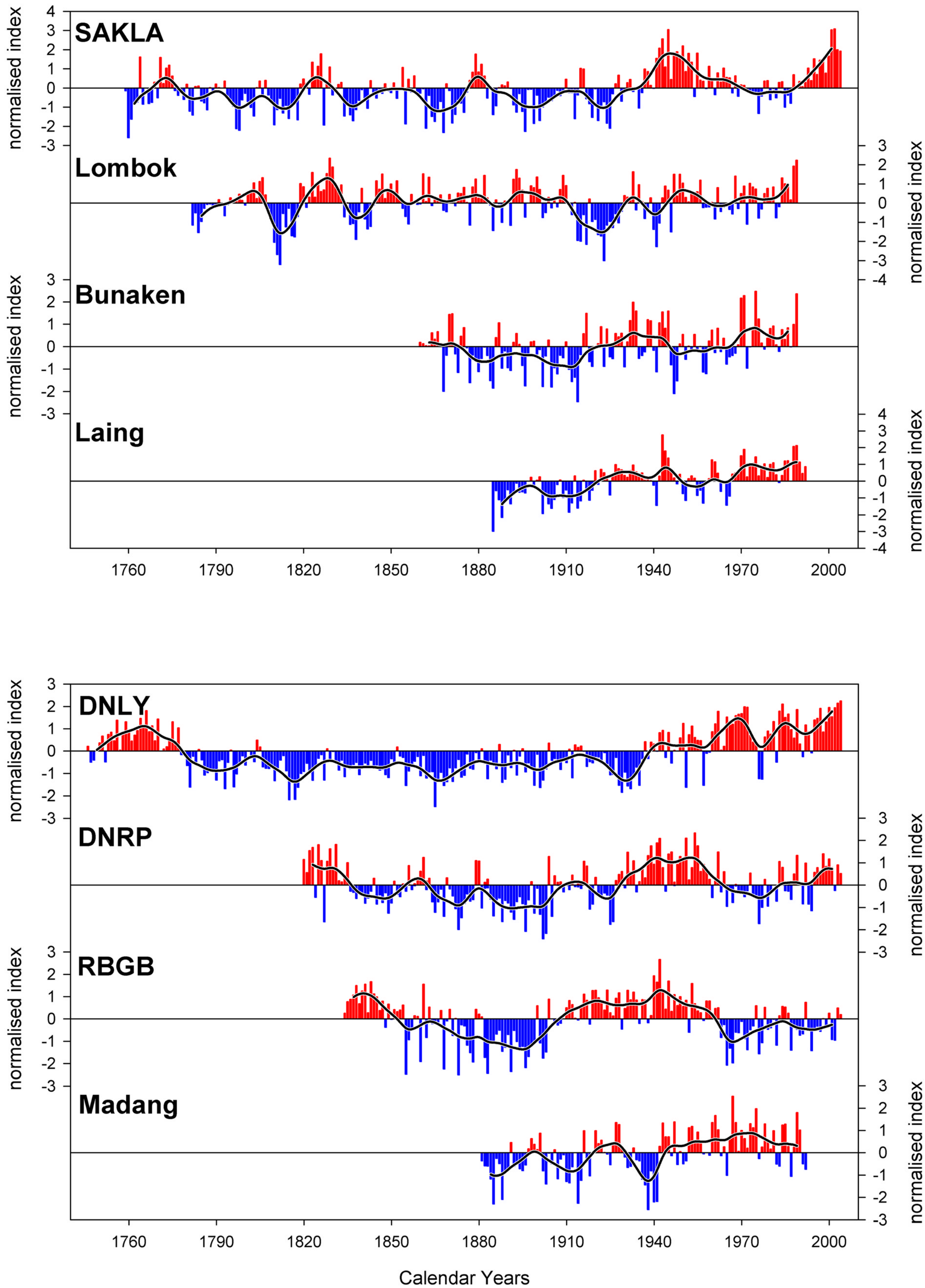
SAKLA
Lombok
Bunaken
Laing
DNLY
DNRP
RBGB
Madang
normalised index
Calendar Years
1760
1790
1820
1850
1880
1910
1940
1970
2000

Figure 2

Table 2. Correlation Matrix Between the Teak and Coral Unfiltered Series That Express a Significant Relationship With Warm Pool SSTs[a]

	SAKLA	DNRP	RBGB	LOM	BUN	MAD	LNG
			DNLY				
Corr	0.35	0.23	0.06[b]	−0.24	−0.26	−0.36	−0.35
p	0.00	0.02	0.54[b]	0.02	0.01	0.00	0.00
			SAKLA				
Corr		0.60	0.39	−0.16[b]	−0.18	−0.15[b]	−0.20
p		0.00	0.00	0.10[b]	0.07[b]	0.12[b]	0.04
			DNRP				
Corr			0.62	−0.14[b]	−0.26	−0.10[b]	−0.22
p			0.00	0.14[b]	0.01	0.31[b]	0.02
			RBGB				
Corr				0.08[b]	−0.21	−0.09[b]	−0.24
p				0.44[b]	0.03	0.38[b]	0.01
			LOM				
Corr					0.32	0.34	0.33
p					0.00	0.00	0.00
			BUN				
Corr						0.39	0.65
p						0.00	0.00
			MAD				
Corr							0.64
p							0.00

[a]Corr is the correlation, and p is the significance.
[b]Correlations not significant at the 95% CL are shaded.

model. The tree ring and coral data were input as potential predictor series in the regression. Only those series that most significantly correlated with the WP SST series entered the final model. Calibration trials (not shown) indicated that the September–November season optimized the SST signal in the combined proxies. These autumn months are an important time for reconstructing SST because they fall within the June to November period when monsoon rainfall over much of Indonesia is most strongly impacted by ENSO, and when this relationship is most spatially coherent [*Aldrian and Susanto*, 2003; *Chang et al.*, 2004].

[8] A variant of a nesting procedure [e.g., *Meko*, 1997; *Cook et al.*, 2002] was employed to maximize the length of the reconstruction. Using this method, iterative stepwise regression-generated nested models of different lengths (due to the loss of the shorter series leaving the data matrix) were generated and the relevant sections spliced together following normalization and scaling to the mean and standard deviation of the most replicated nest. Two nested models were developed, beginning in 1782 (LOM and SAKLA), and 1860 (BUN, LOM, and SAKLA); with a further model to extend the reconstruction to 1992 (LNG and SAKLA). The final nest reconstructions are effectively linear weighted averages of the original series that entered that particular nest model.

[9] Calibration-verification statistics commonly used in dendroclimatology [*Cook and Kairiukstis*, 1990] were performed separately for each nest and utilized to quantify the robustness of the reconstruction over time. These statistics are the reduction of error (RE), coefficient of efficiency (CE), product means (PM), sign test (ST), and Pearson's correlation coefficient [*Cook and Kairiukstis*, 1990]. A split period calibration-verification scheme was applied over the periods 1885–1936 and 1937–1989, with the final reconstruction based on the full calibration model from 1885–1989. The full spliced reconstruction time series (1782–1992) was scaled (same mean and variance [*Esper et al.*, 2005]) to the instrumental data over the 1885–1989 period to account for the possible bias from using OLS regression for calibrating linear relationships, which results in predicted data with lower variance than the original instrumental data [*von Storch et al.*, 2004].

[10] The reconstruction and associated calibration and verification results are presented in Figure 3 and Table 3, respectively. Because of the stepwise approach used to develop the reconstruction, some of the proxy series, despite being significantly correlated with warm pool SSTs, were not included in the final model. The statistical results, which include positive RE and CE values (indications of predictive model skill), reveal that the model is reasonably robust over the full length of the record. Both the CE and Sign Test results are weak for the earliest nest but the RE is still positive, indicating some useful model skill. In addition, and perhaps most importantly due to the weak midfrequency to low-frequency correlations for the tree ring data (Figure 1), there is no significant trend in the model residuals for the various nests based on either the Durbin-Watson test statistic or the linear trend in the model residuals (Table 3). The reconstruction (1782–1992) explains 52% of the variance for the most replicated (1860–1989) nest, with this value dropping to 30% prior to this period (Table 3). As the proxy series are intercorrelated (Table 2), we tested for potential multicollinearity using the variance inflation factor (VIF [*Fox*, 1997]). All VIF values (not shown) are well below the defined threshold of *Fox* [1997], indicating that the amount of explained variance was not artificially inflated due to multicollinearity [*Cook et al.*, 1994]. It should be noted, however, that the coherence between the instrumental data and the reconstruction weakens markedly prior to the mid 1870s (Figure 3b). This may partly reflect the 'quality' of the

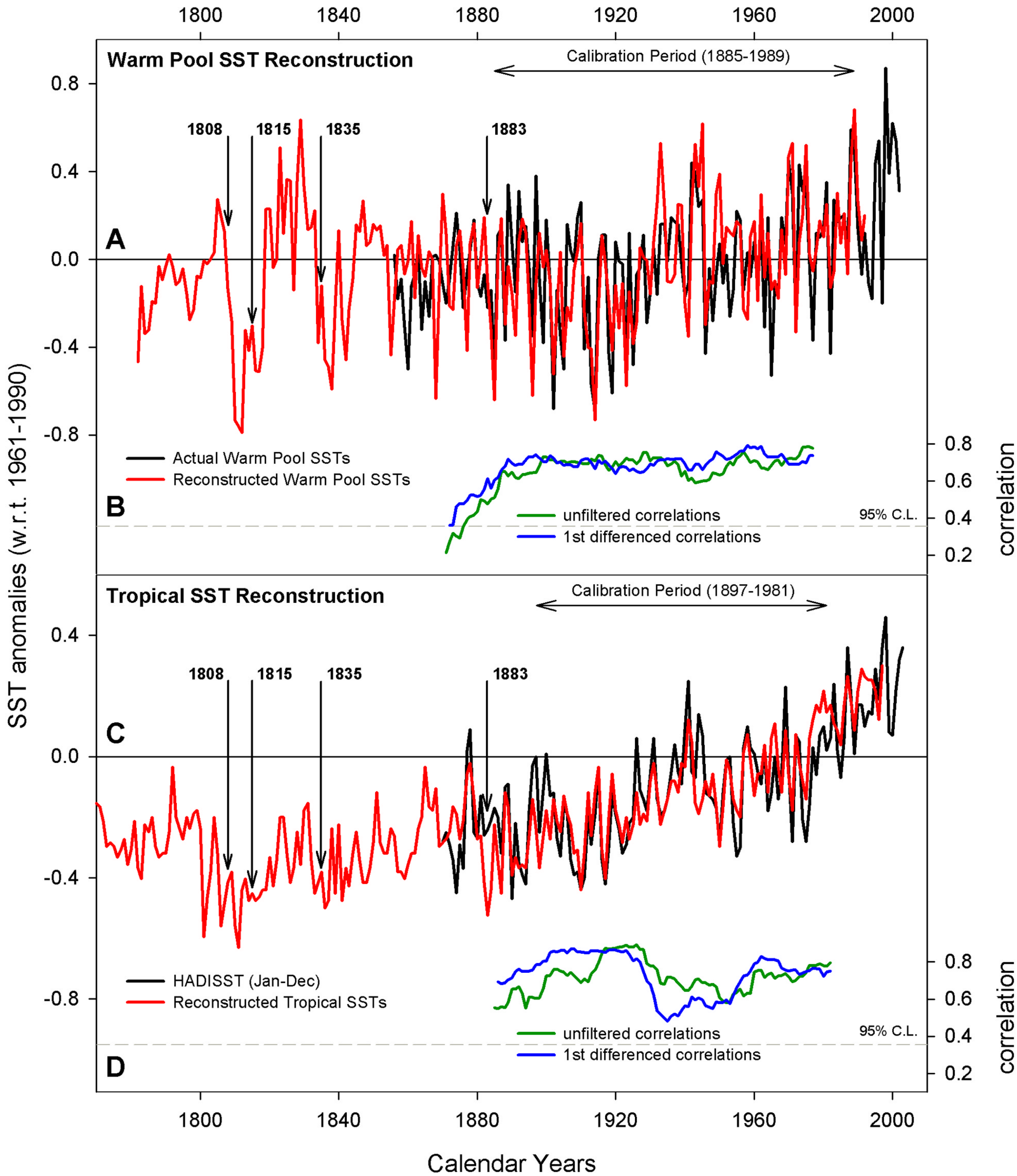

Figure 3. Warm pool reconstruction. (a) Actual (red) and reconstructed (purple) September–November Indonesian warm pool SSTs. Volcanic episodes are indicated with arrows; see text. The reconstructed values have been scaled (same mean and variance [*Esper et al.*, 2005]) to the instrumental data over the 1885–1989 period to account for the possible bias from using OLS regression for calibrating linear relationships, which results in predicted data with lower variance than the original instrumental data [*von Storch et al.*, 2004]. The regression of the proxies against SST calibrates the time series to SST values. (b) Running 31-year correlation plots between the reconstruction and instrumental data. Correlations are calculated for both the unfiltered data (black) and first-differenced transforms (blue). (c and d) Same as Figures 3a and 3b, but for *Wilson et al.* [2006] tropical SST reconstruction.

Table 3. Calibration and Verification Statistics for Nested Reconstruction Models[a]

Calibration			Verification					
Period	r	aR2	Period	r	RE	CE	PM	ST
Splice Period 1990–1992[b]								
1885–1936	0.55	0.30	1937–1989	0.46	0.30	0.06	4.19	36/17
1937–1989	0.60	0.33	1885–1936	0.47	0.37	0.19	3.67	32/20
1885–1989	0.58	0.33						
Splice Period 1860–1989[c]								
1885–1936	0.70	0.46	1937–1989	0.66	0.51	0.34	4.50	43/10
1937–1989	0.73	0.50	1885–1936	0.66	0.56	0.44	3.89	37/15
1885–1989	0.73	0.52						
Splice Period 1782–1859[d]								
1885–1936	0.57	0.30	1937–1989	0.37	0.25	0.00	3.42	40/13
1937–1989	0.54	0.27	1885–1936	0.42	0.30	0.10	3.89	31/21[e]
1885–1989	0.56	0.30						

[a]These results can be used to assess the skill gained by the addition of each proxy predictor. Here r is correlation coefficient; aR^2 is square of the multiple correlation coefficient following adjustment for loss of degrees of freedom; RE is reduction of error statistic; CE is coefficient of efficiency statistic; RE and CE values greater than zero indicate good model skill; there is no significance level per se [*Cook and Kairiukstis*, 1990]; PM is product means test [*Fritts*, 1991]; ST is the sign test [*Fritts*, 1976], showing ratio of agreement/disagreement; values are significant at the 95% confidence level unless otherwise noted; DW is Durbin-Watson statistic for residual autocorrelation; linear r is correlation of linear trend in residual series.

[b]DW = 1.75; linear r = −0.09; proxy variables LNG, SAKLA.

[c]DW = 1.87; linear r = −0.05; proxy variables BUN, LOM, SAKLA.

[d]DW = 1.64; linear r = 0.12; proxy variables LOM, SAKLA.

[e]Not significant at the 95% confidence level.

instrumental data, which is based on relatively few observations during this time [*Kaplan et al.*, 1998]. Some additional confirmation of the earlier period of the reconstruction, however, is provided below through comparison with other climate records. For example, Figure 3c compares the entirely independent coral-based tropical temperature reconstruction of *Wilson et al.* [2006], which shows agreement with the warm pool reconstruction at lower frequencies as well as expressing a common response to some volcanic events (see later).

[11] Warming is evident over the past century in both the instrumental and reconstructed warm pool series (Figure 3a, both series increase by 0.2°C/100 years over the 1856–1992 period). Similarly, warming has been observed for Indonesia [*Harger*, 1995] and over the tropics (30°S–30°N) as a whole [*Wilson et al.*, 2006] (Figure 3c), although over the same period, the rate of increase of mean tropical annual SSTs is marginally greater at 0.3°C/100 years. The famed 1976 climate shift is not clearly evident in either the actual or reconstructed warm pool SST records for the September–November season analyzed herein, despite its presence in a number of climate indices over the equatorial Indo-Pacific as well as the Pacific basin [*Graham*, 1994; *Deser et al.*, 2004]. This finding is consistent with some analyses of Pacific climate that indicate little or no climatic shift at this time over Indonesia [*Graham*, 1994]. Despite the reasonable empirically derived modeling of the warm pool SSTs, we should note that the reconstruction may reflect an unquantifiable salinity bias from the $\delta^{18}O$ records, as well as inconsistencies with regards to trend in some of these

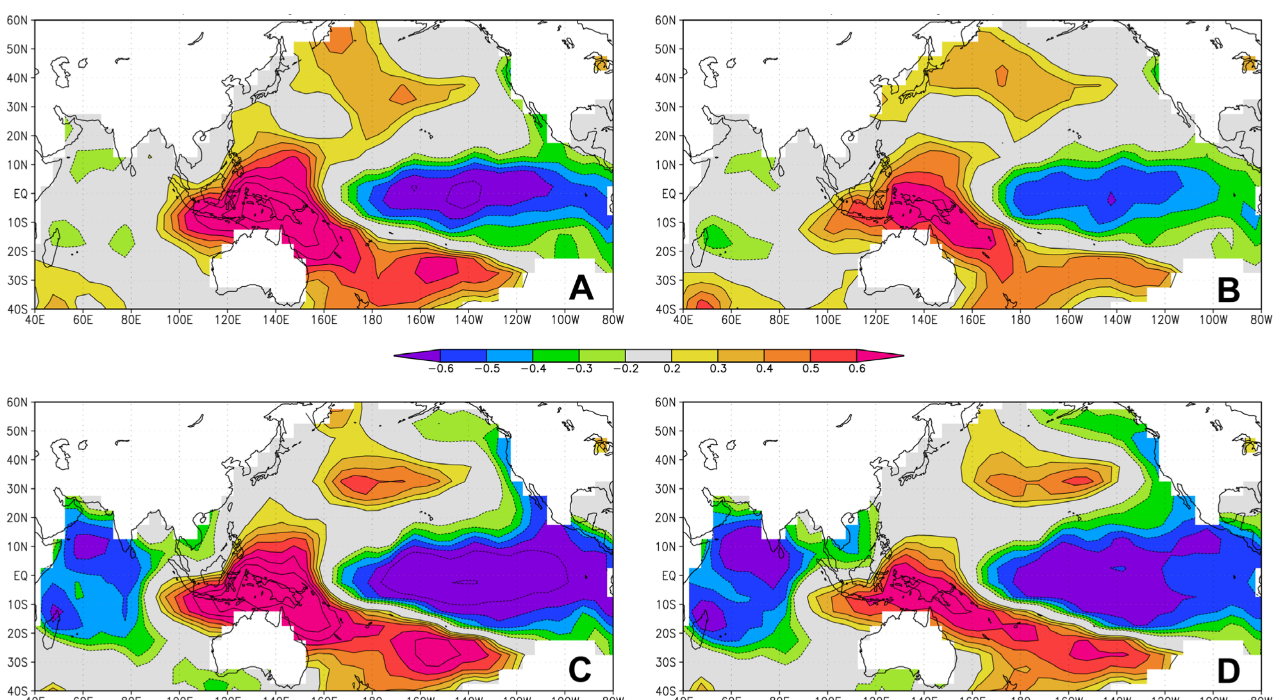

Figure 4. Spatial correlation fields (1885–1989) of (a and c) actual and (b and d) estimated September–October Indonesian warm pool and global SSTs [*Kaplan et al.*, 1998]. Correlations are slightly higher for this season than September–November. Figures 4a and 4b generated using unfiltered data, while Figures 4c and 4d were calculated from first-difference transformed time series.

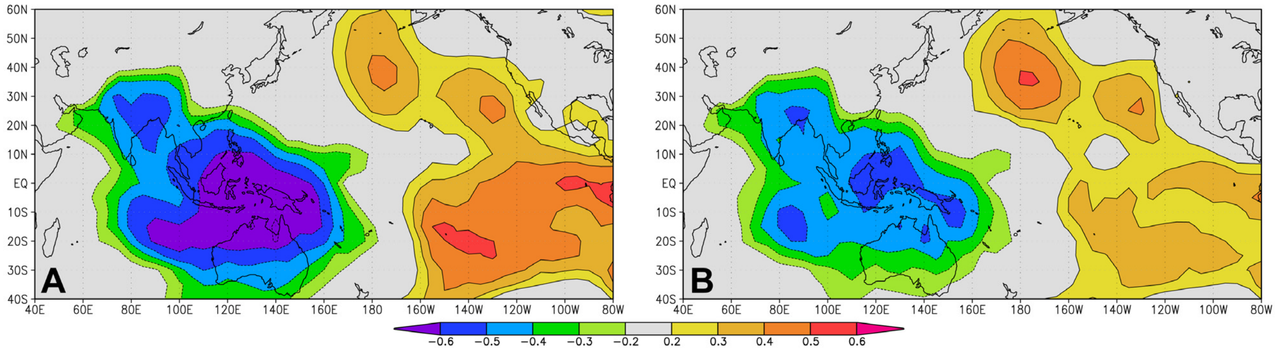

Figure 5. Spatial correlations (1885–1989) of (a) warm pool instrumental and (b) reconstructed September–October warm pool SSTs with Hadley Centre SLP [*Basnett and Parker*, 1997].

series [*D'Arrigo et al.*, 1994; *Moore*, 1995] (see Figure 2). The multiproxy approach that we have used, however, should minimize these biases to some degree. The correlations with local and large-scale SSTs indicate that the proxies are doing well at correlating the large-scale climate signal. This was also observed by *Moore* [1995] and in other relevant coral papers cited herein. The verification statistics would also fail if local site effects dominated the signal in the proxies. Although corals can record changing temperature, light, and salinity effects as they grow to the surface, this is really only an issue for corals living in very shallow water that grow up to the intertidal zone (where the gradients are very steep). The corals used in this study were all substantially subtidal even when cored and did not grow up through any major vertical gradients in their lifespan.

[12] Spatial correlation maps compare the actual and reconstructed warm pool series to the global SST field for the instrumental period (Figure 4) [*Kaplan et al.*, 1998]. Over the calibration period, the proxy estimates, based on both unfiltered and first differenced data, capture the large-scale features seen in the instrumental warm pool SST correlation field, which is dominated by the characteristic ENSO pattern. Interestingly, correlations with Indian Ocean SSTs are only significant for the first-difference comparisons (Figures 4c and 4d), suggesting some differences in low-frequency signals between the Indian Ocean and Indo-

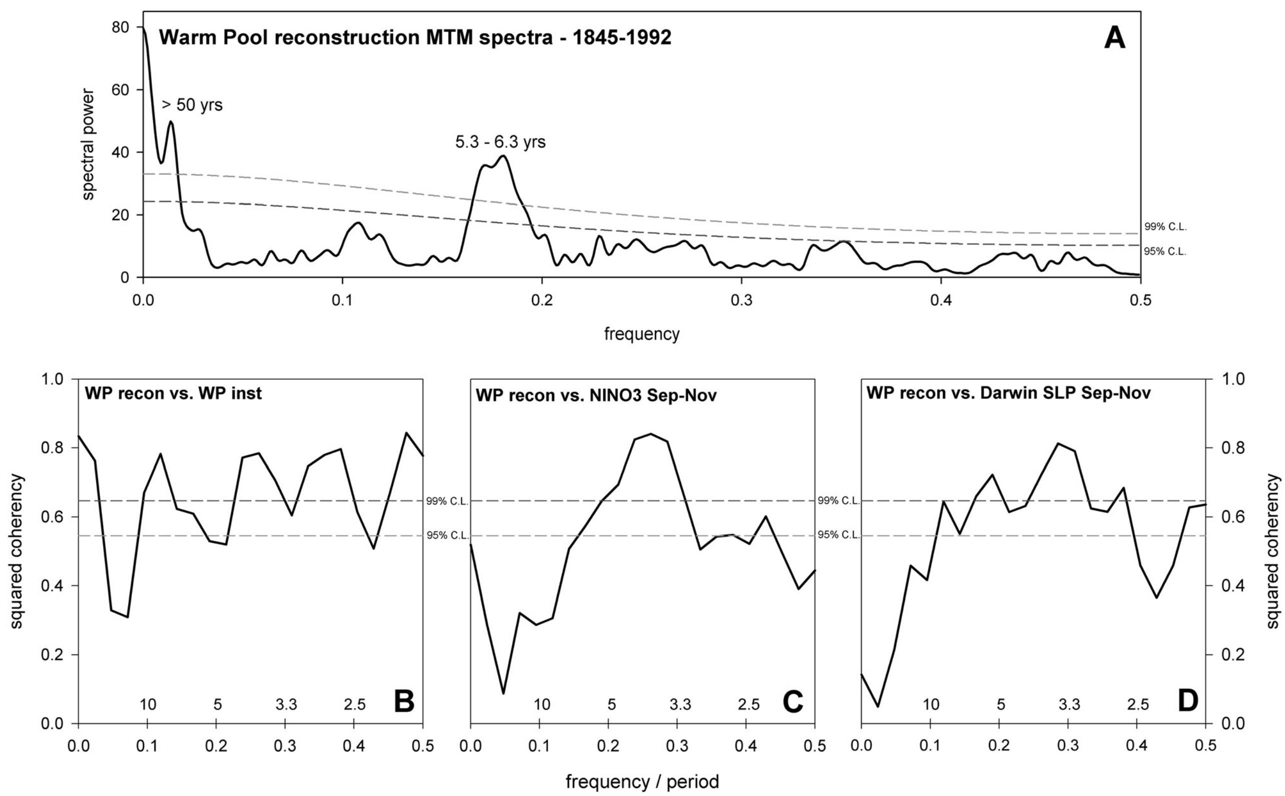

Figure 6. Multitaper method (MTM [*Mann and Lees*, 1996]) spectral analysis of (a) warm pool SST reconstruction and (b–d) coherency spectra with three instrumental climate indices.

Table 4a. Correlations of Instrumental Warm Pool Temperatures With Various Instrumental Climate Indices for the High- and Middle Frequency Bands for the Period 1900–2000[a]

	NINO3	PDO	All India
<10	−0.77[b]	−0.38[b]	0.37[b]
10–30	−0.64[b]	−0.26	0.23

[a]See text. Correlations with Niño-3 (NINO3) SSTs [*Kaplan et al.*, 1998], PDO [*Mantua et al.*, 1997], and all India monsoon index [*Sontakke and Singh*, 1996] are indicated. Niño-3 season is September–November; PDO season is August–October. The significance of the correlations using the smoothed series (i.e., 10–30 and >30 years) was calculated after the degrees of freedom had been adjusted to account for the first-order autocorrelation in the time series [*Dawdy and Matalas*, 1964].
[b]Resultant significance of the correlations for the 99% confidence limits.

Table 4c. Correlations of Reconstructed Warm Pool Temperatures Against Various ENSO Proxy Reconstructions Over the 1900–1976 Period[a]

	Cook	Stahle	Mann	Trop
<10	−0.57[b]	−0.63[b]	−0.44[b]	−0.63[b]
10–30	−0.46[c]	−0.51[c]	−0.45[d]	−0.44[d]
>30	-	-	-	0.88

[a]Proxy ENSO reconstructions are Cook from *D'Arrigo et al.* [2005a], Stahle from *Stahle et al.* [1998], and Mann from *Mann et al.* [2000]. Sign of the Stahle record has been inverted. TROP is coral tropical reconstruction [*Wilson et al.*, 2006]. The degrees of freedom have been adjusted to account for the first-order autocorrelation in the time series [*Dawdy and Matalas*, 1964]. The significance values were calculated as described in Table 4a.
[b]Resultant significance of the correlations for the 99% confidence limits.
[c]Resultant significance of the correlations for the 95% confidence limits.
[d]Resultant significance of the correlations for the 90% confidence limits.

nesian warm pool regions. Evaluation of the instrumental data and reconstruction with the global SLP field (Hadley Centre data set [*Basnett and Parker*, 1997]) show positive correlations over the eastern Pacific, with pronounced negative correlations over Asia in areas impacted by the Australian-Asian and Indian monsoons (Figure 5). These relationships are consistent with the tendency for the Indonesian Low pressure cell to be associated with greater rainfall and warmer SSTs over these regions [*Allan*, 2000].

[13] Multitaper method [*Mann and Lees*, 1996] spectral analysis of the warm pool reconstruction reveals significant spectral peaks at >50 years and in the ENSO band at 5.3–6.3 years (Figure 6a). The ∼5–6 year spectral mode is consistent with those found in previous instrumental studies of ENSO [e.g., *Tourre et al.*, 2001] and in coral data from across the Indo-Pacific [*Moore*, 1995; *Cole et al.*, 2000; *Cobb et al.*, 2001; *Charles et al.*, 2003] and the tropics as a whole [*Wilson et al.*, 2006]. Coherency spectral analysis was performed between the warm pool reconstruction and instrumental warm pool SSTs, Niño-3 SSTs, and Darwin, Australia SLP (Figures 6b–6d). All three analyses demonstrate highly significant (95% level or higher) coherency at periods of ∼2–10 years. The comparison of instrumental and reconstructed warm pool SSTs (Figure 6b) reveals coherency that extends across much of this interval, whereas the coherency is concentrated at ∼4–5 years for Niño-3 SST (Figure 6c) and at ∼3 years for Darwin SLP (Figure 6d).

[14] On the basis of the range of variability shown in these spectral results, we divided the warm pool SST reconstruction into three filtered frequency bands (<10, 10–30, and >30 years) for further analysis. Tables 4a–4d present correlations between the actual and reconstructed warm pool SST series for these frequency bands and a suite of relevant instrumental and proxy climate indices for the tropical Indo-Pacific and vicinity. We focus herein on results for the two higher-frequency bands, and only include the >30 year results for comparison with a coral-based temperature reconstruction for tropical latitudes [*Wilson et al.*, 2006]. Correlations using the instrumental warm pool SST data are significant (99% CL) with instrumental ENSO indices for the past century, as well as with the PDO and an Indian monsoon rainfall index, although with the latter indices, the correlations are weak and non significant at the 10–30 year timescale (Table 4a) [*Sontakke and Singh*, 1996]. Similar results are obtained using the warm pool reconstruction, although correlations with the Pacific Decadal Oscillation (PDO) appear stronger than for the warm pool SST data (r = −0.49 versus −0.38, respectively; these two correlations are not statistically different from each other; Table 4b). Correlations are also significant with several proxy reconstructions of ENSO (Tables 4c and 4d) [*Stahle et al.*, 1998; *Mann et al.*, 2000; *D'Arrigo et al.*, 2005a]. It is perhaps noteworthy to highlight the high correlations with the independent tropical temperature reconstruction noted above (Tables 4a–4d) [*Wilson et al.*, 2006]. However, observe that correlations are negative at higher frequencies and positive at lower frequencies (see below).

3. Warm Pool SST Reconstruction and Extreme Climate Events

[15] The warm pool reconstruction shows a pronounced decade-long cool period between ∼1808 and 1818 (Figure 3). This period corresponds to, and is likely forced

Table 4b. Same as Table 4a But With the Correlations Calculated Using Reconstructed Warm Pool Temperatures Against Various Instrumental Climate Indices[a]

	NINO3	PDO	All India
<10	−0.60[b]	−0.49[b]	0.32[b]
10–30	−0.49[c]	−0.50[c]	0.34

[a]The significance values were calculated as described in Table 4a.
[b]Resultant significance of the correlations for the 99% confidence limits.
[c]Resultant significance of the correlations for the 95% confidence limits.

Table 4d. Same as Table 4c But Calculated Over the 1782–1976 Period[a]

	Cook	Stahle	Mann	Trop
<10	−0.41[b]	−0.47[b]	−0.27[b]	−0.38[b]
10–30	−0.24	−0.35[c]	−0.22	0.09
>30	-	-	-	0.56

[a]The significance values were calculated as described in Table 4a.
[b]Resultant significance of the correlations for the 99% confidence limits.
[c]Resultant significance of the correlations for the 95% confidence limits.

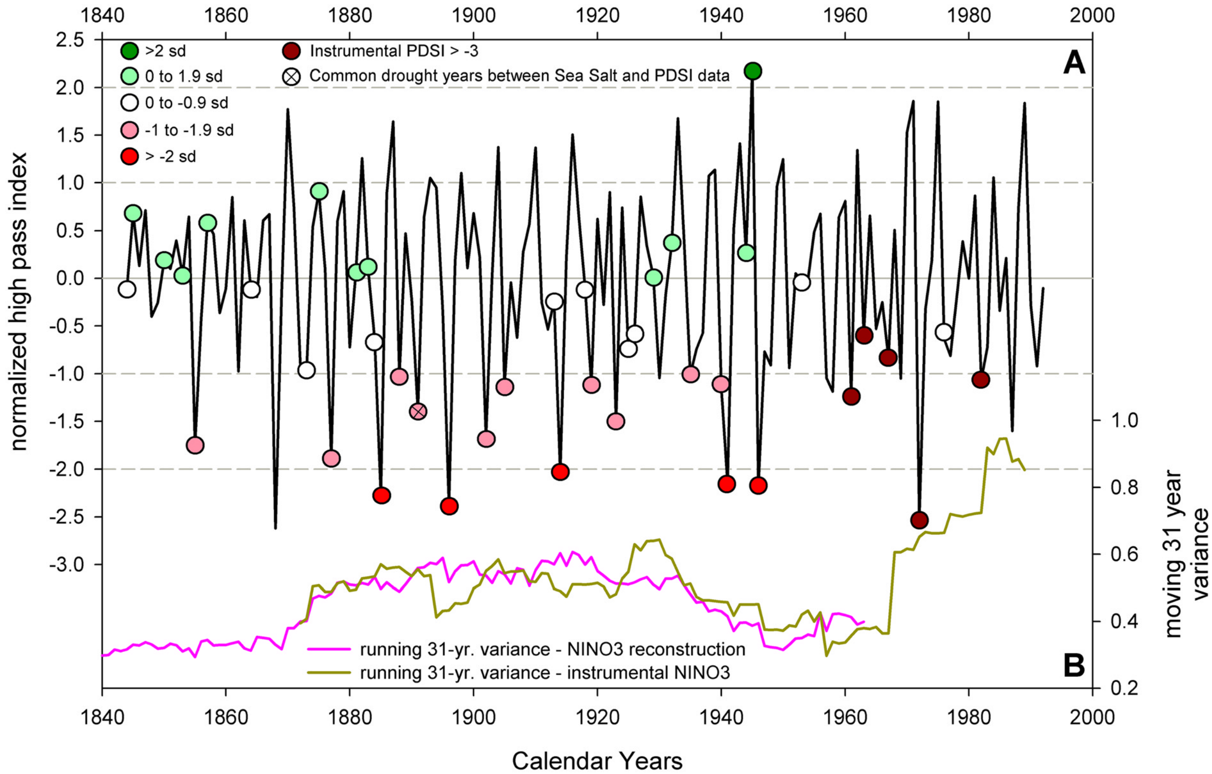

Figure 7. Comparison between the warm pool reconstruction and the sea salt drought record [*Quinn et al.*, 1978]. (a) High-pass-filtered (10 year) normalized warm pool reconstruction. The sea salt events are highlighted with circles and colored relative to the standard deviation values of the coincident year in the reconstruction. Dry years for the recent period are defined using Palmer Drought Severity Index (PDSI) data averaged over Java and vicinity [*Dai et al.*, 2004]. Only extreme (<−3) years are shown. (b) Moving 31-year variance windows of the *D'Arrigo et al.* [2005a] Niño-3 SST reconstruction and instrumental data.

by two major volcanic episodes: an unknown event in 1809 (inferred from sulfate data from Greenland and Antarctic ice cores [*Dai et al.*, 1991]) and the eruption of Tambora, Indonesia in April 1815 [*Simkin and Siebert*, 1994]. Recent ice core results more precisely date the former eruption, which of the two, shows the greatest impact on reconstructed warm pool SSTs, at March–July 1808 [*Cole-Dai and Thompson*, unpublished data]. Both of these eruptions produced highly significant cooling over some tropical regions, including the warm pool area, according to an early data set of global marine air temperature for 1807–1827 [*Chenoweth*, 2001]. Annual marine air temperature anomalies in the tropics (20°N–20°S) were −0.84 (±0.20°C) in 1809 and −0.81 (±0.17°C) in 1816 [*Chenoweth*, 2001]. The cooling observed by *Chenoweth* [2001] during the early 1800s supports the case that much of the shift in the warm pool reconstruction is due to temperature rather than salinity. Reconstructed warm pool anomalies from 1809–1812 are −0.28, −0.73, −0.76, and −0.79°C; and −0.30, −0.51 and −.51°C for 1815–1817 (95% standard error confidence range for each annual value is (±0.46°C). An ENSO warm event ~1817 may have contributed to some of the cooling after Tambora [*Ortlieb*, 2000; *Chenoweth*, 2001].

[16] Elsewhere in Asia, premonsoon and postmonsoon temperature reconstructions for Nepal show conditions around the time of the Tambora event to be the coldest in the past six centuries [*Cook et al.*, 2003]. Madras, India temperatures were also cold, falling from above to well below average by June 1815 [*Chenoweth*, 2001]. There are also pronounced negative anomalies in the warm pool reconstruction following other volcanic events, including the Coseguina, Nicaragua (1835; reconstructed values in 1836–1838 are −0.46, −0.49, and −0.59°C) and Krakatoa, Indonesia eruptions (1883; values for 1883–1885 are −0.11, −0.32, and −0.64°C; Figure 3 [*Simkin and Siebert*, 1994]). Several ENSO events in the 1830s [*Ortlieb*, 2000] could also help explain the cold reconstructed SSTs around the time of the Coseguina event.

[17] In addition to volcanism, the warm pool SST reconstruction shows close correspondence with ENSO and monsoon rainfall indices and extremes (Table 4a and Figure 7). However, it appears insensitive to the severe 1789–1793 episode of warm ENSO conditions and reported monsoon drought over India and Java (reconstructed SST value for mean of 1789–1793 is −0.05). There is a more negative anomaly during the major 1877 ENSO and monsoon drought episode (−0.42°C [*Grove*, 1998]).

[18] The warm pool reconstruction, after high-pass filtering (10 years) and normalizing, was also compared to a listing of east monsoon droughts for Java, Indonesia, compiled from historical sea salt records from Dutch estates (1844–1976, Figure 7 [*Quinn et al.*, 1978]). This comparison allows some additional evaluation of the reconstruction using land-based historical data. During periods when ENSO variability is low (based on *D'Arrigo et al.*'s [2005a] Niño-3 SST reconstruction), there appears to be little relationship between drought events [*Quinn et al.*, 1978] and warm pool reconstructed SSTs. For example, over the periods ~1844–1875 and ~1929–1960, periods with relatively low interannual variance in ENSO (Figure 7b) [*Allan*, 2000; *D'Arrigo et al.*, 2005b], the median normalized SST departures are 0.03 (standard deviation 0.84, 9 cases) and −0.04 (standard deviation 1.37, nine cases), respectively. However, the reconstruction is more consistent with the sea salt record from 1877 to 1926, a period of greater variability with several relatively strong ENSO warm events, when the reconstructed normalized departure is −1.11 (standard deviation 0.80, 17 cases). Agreement during the relatively weak early and late periods is better for some individual ENSO events, e.g., in 1941 when the normalized SST departure is −2.14. The year 1868, coincident with a moderate to strong ENSO warm event [*Ortlieb*, 2000], has one of the years of lowest reconstructed warm pool SSTs on record; however it is not listed as a drought year in the historical sea salt information. There is also good agreement in the recent instrumental period when the warm pool reconstruction is compared to an instrumental drought index for Java and vicinity (Palmer Drought Severity Index or PDSI [*Dai et al.*, 2004]; see *D'Arrigo et al.* [2006] for a description of a PDSI reconstruction for Java, Indonesia). These results suggest that there is greater coupling of Javan drought and warm pool SSTs during periods of strong ENSO variability.

[19] With regards to other tropical proxies, significant departures are also evident in the Malindi coral $\delta^{18}O$ record from the far western Indian Ocean during both the unknown and Tambora early 1800s episodes, as well as other volcanic events [*Cole et al.*, 2000]. Responses to volcanism are also noted in an independent coral-based reconstruction of tropical SSTs [*Wilson et al.*, 2006] (Figure 3c). This latter record shows significant cooling in tropical SSTs related to the 1808 and 1883 events. Little response is noted however, to the 1815 event, possibly because the ENSO warm episode ~1817 may have counteracted some of the cooling after Tambora in some areas of the tropics [*Ortlieb*, 2000; *Chenoweth*, 2001]. Most of the coral records utilized by *Wilson et al.* [2006] are situated in the central Pacific (although Malindi was also included), and therefore express a strong positive response to high-frequency ENSO variability. The relationship between the warm pool and tropical temperature reconstructions is thus inverse at high frequencies (despite the common response to some volcanic events, Figure 3c), due to their inverse high-frequency response to ENSO (Tables 4a–4d). The mid to high-frequency information in the warm pool reconstruction, at least recently, appears to also be controlled by ENSO, and/or PDO-related dynamics. However, the fact that the low-frequency (>30 years) mode is positively correlated between the warm pool and tropical temperature reconstructions begs the question as to what is the ultimate control (possibly solar or anthropogenic forcing) at these secular frequencies.

4. Summary

[20] We have described a reconstruction of SST for the Indonesian warm pool region based on tree ring and coral data. This study is among the first to reconstruct high-resolution tropical climate variability based on combined terrestrial and marine proxies from the equatorial tropics. Both proxies contribute important, independent information to the reconstruction. The reconstruction is robust, capturing 52% of the instrumental variance over the most replicated period, with significant calibration and verification statistics. It demonstrates both interannual and decadal fluctuations that appear related to ENSO and/or Pacific decadal variability. There is highly significant coherency between the reconstruction, instrumental warm pool SSTs, Niño-3 SST and Darwin SLP data. When separated into three frequency bands, we observe correspondence between the warm pool series and both instrumental and proxy indices of Indo-Pacific and Pacific basin climate. Coincidence between anomalously cold warm pool temperatures in the early 1800s and major volcanic events confirms previous findings of pronounced lowering of tropical marine air temperatures in early instrumental observations [*Chenoweth*, 2001], and helps quantify the impact of these events on the warm pool region. There is some agreement between anomalous years in the reconstruction and those found in records of Asian monsoon rainfall during major ENSO episodes. However, we caution that the reconstruction is based on relatively few proxy series and extends back for little more than two centuries. There are efforts underway to extend the living teak record back in time using subfossil wood, although the degree to which this is possible is constrained by the date at which teak was introduced to Indonesia (possibly as much as 1000 years ago). Living corals are also limited in their longevity, although there has been success using subfossil samples to reconstruct selected time slices [e.g., *Cobb et al.*, 2003]. Trends are also somewhat uncertain as there are local factors at play in addition to the regional signals. Consequently, additional records are needed to improve our understanding of the behavior of the Indonesian warm pool and the factors, including ENSO, that impact its variability.

[21] **Acknowledgments.** This project was funded by the National Science Foundation Paleoclimate Program (grant OCE 04-02474). Rob Wilson and Alexander Tudhope are partly funded by the European Union Project "Simulations, Observations and Palaeoclimatic data" (SOAP) and by the UK NERC. We thank G. Dunbar and two anonymous reviewers for comments that significantly improved the manuscript. We thank M. Moore and C. Charles for providing data and also gratefully acknowledge the Indonesian Institute of Sciences (LIPI) and contributors to the NOAA Paleoclimatology Data Bank. Some plots were generated using KNMI Climate Explorer. Lamont-Doherty Earth Observatory contribution 6895.

References

Aldrian, E., and R. Susanto (2003), Identification of three dominant rainfall regions within Indonesia and their relationship to sea surface temperature, *Int. J. Climatol.*, *23*, 1435–1452.

Allan, R. J. (2000), ENSO and climatic variability in the past 150 years, in *ENSO: Multiscale Variability and Global and Regional Impacts*, edited by H. F. Diaz and V. Markgraf, pp. 3–55, Cambridge Univ. Press, New York.

Barlow, M., H. Cullen, and B. Lyon (2002), Drought in central and southwest Asia, La Niña, the warm pool and Indian Ocean precipitation, *J. Clim.*, *15*, 697–700.

Basnett, T., and D. Parker (1997), Development of the Global Mean Sea Level Pressure Data Set GMSLP2, *Clim. Res. Tech. Note*, *79*, Hadley Centre, Met Office, Exeter, U. K.

Chang, C.-P., Z. Wang, J. Ju, and T. Li (2004), On the relationship between Western Maritime Continent monsoon rainfall and ENSO during northern winter, *J. Clim.*, *17*, 665–672.

Charles, C., D. Hunter, and R. Fairbanks (1997), Interaction between the ENSO and the Asian monsoon in a coral record of tropical climate, *Science*, *277*, 925–928.

Charles, C. D., K. Cobb, M. D. Moore, and R. G. Fairbanks (2003), Monsoon-tropical ocean interaction in a network of coral records spanning the 20th century, *Mar. Geol.*, *201*, 207–222.

Chenoweth, M. (2001), Two major volcanic cooling episodes derived from global marine air temperature, AD 1807–1827, *Geophys. Res. Lett.*, *28*, 2963–2966.

Cobb, K., C. Charles, and D. Hunter (2001), A central tropical Pacific coral demonstrates Pacific, Indian, and Atlantic decadal climate connections, *Geophys. Res. Lett.*, *28*, 2209–2212.

Cobb, K., C. Charles, H. Cheng, and R. Edwards (2003), El Niño–Southern Oscillation and tropical Pacific climate during the last millennium, *Nature*, *424*, 271–274.

Cole, J., R. Dunbar, T. McClanahan, and N. Muthiga (2000), Tropical Pacific forcing of decadal SST variability in the western Indian Ocean over the past two centuries, *Science*, *287*, 617–619.

Cook, E., and L. Kairiukstis (1990), *Methods of Dendrochronology*, Springer, New York.

Cook, E., and K. Peters (1997), Calculating unbiased tree-ring indices for the study of climatic and environmental change, *Holocene*, *7*, 361–370.

Cook, E. R., K. Briffa, and P. Jones (1994), Spatial regression methods in dendroclimatology: A review and comparison of two techniques, *Int. J. Climatol.*, *14*, 379–402.

Cook, E., R. D'Arrigo, J. Cole, D. Stahle, and R. Villalba (2000), Tree-ring records of past ENSO variability and forcing, in *ENSO: Multiscale Variability and Global and Regional Impacts*, edited by H. F. Diaz and V. Markgraf, pp. 297–323, Cambridge Univ. Press, New York.

Cook, E., R. D'Arrigo, and M. E. Mann (2002), A well-verified, multiproxy reconstruction of the winter North Atlantic Oscillation index since A. D. 1400, *J. Clim.*, *15*, 1754–1764.

Cook, E., P. Krusic, and P. Jones (2003), Dendroclimatic signals in long tree-ring chronologies from the Himalayas of Nepal, *Int. J. Climatol.*, *23*, 707–732.

Dai, J., E. Mosley-Thompson, and L. Thompson (1991), Ice core evidence for an explosive tropical eruption 6 years preceding Tambora, *J. Geophys. Res.*, *96*, 17,361–17,366.

Dai, A., K. E. Trenberth, and T. Qian (2004), A global data set of Palmer drought severity index for 1870–2002: Relationship with soil moisture and effects of surface warming, *J. Hydrometeorol.*, *5*, 1117–1130.

D'Arrigo, R. D., G. C. Jacoby, and P. J. Krusic (1994), Progress in dendroclimatic studies in Indonesia, *TAO*, *5*, 349–363.

D'Arrigo, R., E. R. Cook, R. J. Wilson, R. Allan, and M. E. Mann (2005a), On the variability of ENSO over the past six centuries, *Geophys. Res. Lett.*, *32*, L03711, doi:10.1029/2004GL022055.

D'Arrigo, R., R. Wilson, C. Deser, G. Wiles, E. Cook, R. Villalba, S. Tudhope, J. Cole, and B. Linsley (2005b), Tropical-North Pacific climate linkages over the past four centuries, *J. Clim.*, *18*, 5253–5265.

D'Arrigo, R., R. Wilson, J. Palmer, P. Krusic, A. Curtis, J. Sakulich, S. Bijaksana, S. Zulaikah, and O. Ngkoimani (2006), Monsoon drought over Java, Indonesia during the past two centuries, *Geophys. Res. Lett.*, *33*, L04709, doi:10.1029/2005GL025465.

Dawdy, D. R., and N. C. Matalas (1964), Statistical and probability analysis of hydrologic data, part III: Analysis of variance, covariance and time-series, in *Handbook of Applied Hydrology, A Compendium of Water-Resources Technology*, edited by V. T. Chow, pp. 8.68–8.90, McGraw-Hill, New York.

Deser, S., A. Phillips, and J. Hurrell (2004), Pacific interdecadal climate variability: Linkages between the tropics and North Pacific during boreal winter since 1900, *J. Clim.*, *17*, 3109–3124.

Emanuel, K. (2005), Increasing destructiveness of tropical cyclones over the past 30 years, *Nature*, *436*, doi:10.1038/nature03906.

Esper, J., D. Frank, R. J. S. Wilson, and K. Briffa (2005), Effect of scaling and regression on reconstructed temperature amplitude for the past millennium, *Geophys. Res. Lett.*, *32*, L07711, doi:10.1029/2004GL021236.

Evans, M., M. Cane, D. Schrag, A. Kaplan, B. Linsley, R. Villalba, and G. Wellington (2001), Support for tropically-driven Pacific decadal variability based on paleoproxy evidence, *Geophys. Res. Lett.*, *28*, 3689–3692.

Evans, M. N., A. Kaplan, and M. A. Cane (2002), Pacific sea surface temperature field reconstruction from coral $\delta^{18}O$ data using reduced space objective analysis, *Paleoceanography*, *17*(1), 1007, doi:10.1029/2000PA000590.

Fox, J. (1997), *Applied Regression Analysis, Linear models, and Related Methods*, Sage, London.

Fritts, H. (1976), *Tree Rings and Climate*, Elsevier, New York.

Fritts, H. (1991), *Reconstructing Large-scale Climatic Patterns from Tree-Ring Data: A Diagnostic Analysis*, Univ. of Ariz. Press, Tucson.

Graham, N. (1994), Decadal-scale climate variability in the tropical and North Pacific during the 1970s and 1980s: Observations and model results, *Clim. Dyn.*, *10*, 135–162.

Grove, R. (1998), Global impact of the 1789–93 El Niño, *Nature*, *393*, 318–319, doi:10.1038/30636.

Harger, J. (1995), Air temperature variations and ENSO effects in Indonesia, the Philippines and El Salvador. ENSO patterns and changes from 1866–1993, *Atmos. Environ.*, *29*, 1919–1942.

Hoerling, M., J. Whitaker, A. Kumar, and W. Wang (2001), The mid-latitude warming during 1998–2000, *Geophys. Res. Lett.*, *28*, 755–758.

Holmes, R. L. (1983), Computer-assisted quality control in tree-ring dating and measurement, *Tree Ring Bull.*, *43*, 69–78.

Kaplan, A., M. Cane, Y. Kushnir, A. Clement, M. Blumenthal, and B. Rajagopalan (1998), Analyses of global sea surface temperature 1856–1991, *J. Geophys. Res.*, *103*, 18,567–18,589.

Linsley, B. K., G. M. Wellington, and D. P. Schrag (2000), Decadal sea surface temperature variability in the subtropical South Pacific from 1726 to 1997 A. D., *Science*, *290*, 1145–1148.

Linsley, B., G. Wellington, D. Schrag, L. Ren, M. Salinger, and A. Tudhope (2004), Geochemical evidence from corals for changes in the amplitude and spatial pattern of South Pacific interdecadal climate variability over the last 300 years, *Clim. Dyn.*, *22*, 1–11.

Lough, J. (2004), A strategy to improve the contribution of coral data to high-resolution, *Palaeogeogr. Palaeoclimatol. Palaeoecol.*, *204*, 115–143.

Mann, M. E., and J. Lees (1996), Robust estimation of background noise and signal detection in climatic time series, *Clim. Change*, *33*, 409–445.

Mann, M. E., R. S. Bradley, and M. K. Hughes (2000), Long-term variability in the ENSO and associated teleconnections, in *ENSO: Multiscale Variability and Global and Regional Impacts*, edited by H. F. Diaz and V. Markgraf, pp. 357–412, Cambridge Univ. Press, New York.

Mantua, N., S. Hare, Y. Zhang, J. Wallace, and R. Francis (1997), A Pacific interdecadal oscillation with impacts on salmon production, *Bull. Am. Meteorol. Soc.*, *78*, 1069–1079.

Meko, D. M. (1997), Dendroclimatic reconstruction with time varying subsets of tree indices, *J. Clim.*, *10*, 687–696.

Moore, M. (1995), Proxy records of the Indonesian Low and the El Niño–Southern Oscillation (ENSO) from stable isotope measurements of Indonesian reef corals, Ph.D. dissertation, Univ. Calif., Berkeley.

Ortlieb, L. (2000), The documented historical record of El Niño events in Peru: An update of the Quinn record (sixteenth through nineteenth centuries), in *El Niño and the Southern Oscillation: Multiscale Variability and Global and Regional Impacts*, edited by H. Diaz and V. Markgraf, pp. 207–295, Cambridge Univ. Press, New York.

Quinn, W., D. Zopf, K. Short, and R. Yang (1978), Historical trends and statistics of the Southern Oscillation, El Niño, and Indonesian droughts, *Fish. Bull.*, *76*, 663–678.

Schneider, N. (1998), The Indonesian Throughflow and the global climate system, *J. Clim.*, *11*, 676–689.

Simkin, T., and L. Siebert (1994), *Volcanoes of the World*, 2d ed., 349 pp., Geosci. Press, Tucson, Ariz.

Sontakke, N., and N. Singh (1996), Longest instrumental regional and all-India summer monsoon rainfall series using optimum observations: Reconstruction and update, *Holocene*, *6*, 315–331.

Stahle, D. W., et al. (1998), Experimental dendroclimatic reconstruction of the Southern Oscillation, *Bull. Am. Meteorol. Soc.*, *79*, 2137–2152.

Sun, D. (2003), A possible effect of an increase in the warm-pool SST on the magnitude of El Niño warming, *J. Clim.*, *16*, 185–205.

Tourre, Y., B. Rajagopalan, Y. Kushnir, M. Barlow, and W. White (2001), Patterns of coherent decadal and interdecadal climate signals in the Pacific basin during the 20th century, *Geophys. Res. Lett.*, *28*, 2069–2072.

Tudhope, A., C. Chilcott, M. McCulloch, E. Cook, J. Chappell, R. Ellam, D. Lea, J. Lough, and G. Shimmield (2001), Variability in the El Niño–Southern Oscillation through a glacial-interglacial cycle, *Science*, *291*, 1511–1517.

von Storch, H., E. Zorita, J. Jones, Y. Dimitriev, F. González-Rouco, and S. Tett (2004), Reconstructing past climate from noisy data, *Science*, *306*, 679–682, doi:10.1126/science.1096109.

Wang, B., and X. Xie (1998), Coupled modes of the warm pool climate system. part I: The role of air-sea interaction in Madden-Julian Oscillations, *J. Clim.*, *11*, 2116–2135.

Wilson, R., S. Tudhope, P. Brohan, T. Osborn, K. Briffa, and S. Tett (2006), 250 years of reconstructed and modeled tropical temperatures, *J. Geophys. Res.*, doi:10.1029/2005JC003188, in press.

S. Bijaksana, Department of Physics, Institut Teknologi Bandung, Jalan Ganesha 10 Bandung, Indonesia 40132.

R. D'Arrigo, A. Curtis, P. Krusic, and J. Sakulich, Tree-Ring Lab, Lamont-Doherty Earth Observatory, 61 Route 9W, Palisades, NY 10964, USA. (rdd@ldeo.columbia.edu)

L. O. Ngkoimani, Jurusan Fisika FMIPA, Universitas Haluoleo, Kendari, Southeast Sulawesi, Indonesia 93232.

J. Palmer, Department of Archaeology and Palaeoecology, Lincoln University, P.O. Box 64, Ellesmere Junction Road/Springs Road, Canterbury, New Zealand 8150.

A. Tudhope and R. Wilson, School of Geosciences, University of Edinburgh, West Mains Road, Edinburgh EH9 3JW, UK.

S. Zulaikah, Department of Physics, State University of Jakarta, Jl. Rawamangun Muka, Jakarta, Indonesia 13220.